NASA

Technical Memorandum 82143

Rapid X-Ray Variability in the Seyfert Galaxy NGC 6814.

A.F. Tennant, R.F. Mushotzky, E.A. Boldt and J.H. Swank

JUNE 1981

National Aeronautics and Space Administration

Goddard Space Flight Center
Greenbelt, Maryland 20771

RAPID X-RAY VARIABILITY IN THE SEYFERT GALAXY NGC 6814[1]

A.F. TENNANT[2], R.F. MUSHOTZKY, E.A. BOLDT and J.H. SWANK

Laboratory for High Energy Astrophysics

NASA/Goddard Space Flight Center

Greenbelt, Maryland 20771

ABSTRACT

We report HEAO-1 A-2 high time resolution X-ray observations of the X-ray emitting Seyfert I Galaxy NGC 6814. In sharp distinction with a sample of over 30 active galactic nuclei (Tennant et al. 1981) this object showed strong X-ray variability on timescales less than 3 hours. The mean flux on a timescale of 90 minutes varied by a factor of $\sim$ 2.5 corresponding to $\Delta L_x \sim 1 \times 10^{43}$ ergs/sec. An autocorrelation analysis shows a characteristic time for variability of 100^{+60}_{-25} seconds. There is no indication of spectral variability with an upper limit on a change in the power law spectral index of $|\Delta\Gamma| \lesssim .37$, for a factor two change in intensity. We consider in detail the constraints of such rapid variability on a wide variety of X-ray source mechanisms.

Subject headings: galaxies: individual - galaxies: Seyfert - X-rays: sources

[1]From a dissertation to be submitted to the Graduate School, University of Maryland, by Allyn F. Tennant in partial fulfillment of the requirements for the Ph.D. degree in Physics.

[2]Also Dept. Physics and Astronomy, Univ. of Maryland

I. INTRODUCTION

X-ray observations of the time variability and spectra of active galactic nuclei (AGN) relate directly, in the present conventional wisdom, to the engine responsible for the enormous luminosities of these objects. In particular, observations of rapid X-ray variability place strong constraints on the size of the "central engine", information which is difficult to obtain from observations in the radio, infrared, optical or ultra-violet bands.

Various models of the energy generation mechanism in AGN's have centered (Fabian 1979) on the existence of a compact object in the nucleus of these galaxies. Indirect arguments and various scaling laws indicate that this putative central object has an effective scale size of less than 10^{15} cm (Fabian 1979). Such an object would be revealed by characteristic time variability of less than one day. A general constraint on the fastest timescales expected has been proposed by Fabian and Rees (1979), building on work by Cavallo and Rees (1978). If a spherically symmetric, homogeneous, cloud of stationary matter is converted into radiation with efficiency η, the shortest observed timescale for the conversion occurs when the optical depth of the cloud is unity. This gives a minimum timescale $\Delta\tau_{min} \sim 5\ L_{43}/\eta$ sec, where L_{43} is the luminosity in units of 10^{43} ergs/sec. Typical AGN's have $L_{43} \geq 1$ and, if η is as large as 0.1, timescales as short as 50 sec are possible. On the other hand models of accretion disks (Shapiro, Lightman and Eardley 1976) indicate that most of the X-ray luminosity would come from a region of size $R_x \sim 10\ \frac{GM}{c^2}$. If the luminosity of these objects is Eddington limited then $R_x \sim 10^{11}\ L_{43}$ cm for a characteristic time of $\sim 4\ L_{43}$ sec. Clearly X-ray observations capable of measuring timescales in the 1-10,000 sec time range will sample the predicted characteristic times of the "central engine" in AGN's. Previous X-ray observations of time variability in AGN's

have been prevented from sampling such short timescales by a combination of low source flux, low effective area and relatively high internal background. For only a few objects, NGC 4151 (Tananbaum et al. 1978), Cen-A (Delvaille, Epstein and Schnopper 1978), and NGC 4051 (Marshall et al. 1981) are there reported timescales less than 6 hours. In addition, Tananbaum (1980) has reported timescale of ~ 6 hour for NGC 6814.

In this paper we report the detection of short timescale fluctuations ($t < 1$ hr) in the X-ray flux from the Seyfert I galaxy NGC 6814. This observation is the result of a larger program to look for short term variability from AGN's, the results of which will be reported elsewhere (Tennant et al. 1981).

II. OBSERVATIONS AND DATA ANALYSIS

The GSFC detectors on the HEAO-1[+] satellite have been described in

[+]The A2 experiment on HEAO-1 is a collaborative effort led by E. Boldt of GSFC and G. Garmire of CIT, with collaborators at GSFC, CIT, JPL and UCB.

detail by Rothschild et al. 1979. Because of the peculiarity of our results and the importance of ensuring their validity we describe in Appendix A the analysis procedure used to derive the NGC 6814 data.

Briefly, the observations of NGC 6814 were performed by the HEAO-1 satellite experiment A-2 on April 28 of 1978 from 0 hours UT to 8 hours UT while the satellite was in the pointed mode. Counting rates were returned every 5.12 sec from 8 "independent" counters. Background was determined from deep exposures of "source free" regions of the sky where no sources of flux > 2×10^{-11} ergs/cm^2/sec were seen. The net counting rate was corrected for the effective exposure of the detectors to the source. The rates from the

different detectors could then be summed together to construct a "light curve", with the best available statistics.

In Appendix A we discuss the wide variety of checks made in order to ascertain that the strong variability seen in NGC 6814 was not a result of instrumental problems. We conclude that NGC 6814 is the source of the variable X-ray flux detected with HEAO-1 A-2.

III. RESULTS

Examination of Figure 1 shows that the flux from NGC 6814 is strongly variable. On an orbit-by-orbit (1.5 hour) basis the flux varies by a factor of $\sim$ 2.5 (Table 1). In Table 1 we also show the χ^2 calculated on the assumption that the source was constant during each individual orbit. For all but one of these orbits the value of χ^2 allows us to reject the hypothesis of source constancy on timescales less than 1.5 hours at > 99.99% confidence. This is clearly shown in Figure 2 in which a prominent flux change on a timescale of less than 500 seconds is evident.

Having established source variability on timescales less than 1.5 hours we now attempt to characterize the nature and timescale of this variability.

A. Timescale of variability

The autocorrelation function (ACF) was computed for the first and second orbits using a 10.24 sec bin size. In Appendix B we discuss how the ACF was generated and how errors in the reported timescales were determined. The inferred characteristic timescale of the source intensity and the errors are given in Table 2 for these orbits and the entire data stream. All the data are consistent with a characteristic time of $\sim$ 100 seconds. There was insufficient data for orbits 3-5 for a meaningful autocorrelation function to be calculated separately. In Figure 3a we show the ACF for the complete data set (orbits 1-5 inclusive). The characteristic time for variability is the

slope of the natural logarithm of the ACF (Figure 3b). In panels 3c and 3d are shown, respectively, the "detrended" ACF function and its natural logarithm for the same data (see Appendix B for details). The timescale of 100 seconds seen when the data are "detrended" confirms that this is a characteristic time for the entire data set.

An exponential ACF could be interpreted in terms of a shot noise model. However, we note that many other processes give similar ACF's especially when there is a large amount of statistical noise in the data. In addition, it is quite clear from Figure 1 that the shot parameters change from orbit to orbit. A final note is that a shot noise model is only a method of parameterizing the data and does not necessarily have any physical significance.

B. Limits on Spectral Variability

We have searched for spectral variability in four different ways. 1) We have computed the mean spectrum on an orbit by orbit basis. 2) We have sorted the data on the value of their flux and have computed a mean "hardness" ratio for each value of the flux. 3) We have computed the cross-correlation function between two energy bands. 4) We have looked for spectral variability during a given event. Each of these methods is most sensitive to different types of spectral change as discussed below.

1. Orbit-by-Orbit Variability

The best fit spectra on an orbit-by-orbit basis assuming a power law model of photon index Γ and equivalent column density of hydrogen in the line of sight N_H are shown in Table 3 (all errors are 1σ). These values are to be compared with the flux weighted average for the entire observation of $\Gamma = 1.73 \pm .22$, $N_H = 4.3^{+2.7}_{-2.0} \times 10^{22}$ cm^{-2} (Mushotzky et al. 1980) (90% confidence error). The value of χ^2 computed on the assumption that Γ and N_H for each

orbit is the same as the flux weighted mean is 6.8 for 10 parameters of interest. This indicates that, despite a factor of 2 change in intensity on a timescale of 1.5 hours, the time averaged spectrum did not vary significantly.

If we assume that N_H did not vary during this observation (consistent with the values in Table 3) and fix N_H at the value derived for the entire observation, the formal error in Γ decreases. In Table 4 we show the best fit values of Γ for each orbit under this assumption. There is a slight indication that the source spectrum is marginally flatter when the flux is higher. In Figure 4 we plot Γ vs the 2-20 keV flux on an orbit-by-orbit basis and find that a linear relation of the form $\Gamma = mF+b$ (where F is the flux) gives an acceptable fit with $m = -.054\ ^{+.022}_{-.032}$. This trend is significant at only 2.5σ however. Alternatively we place a 3σ upper bound of $\Delta\Gamma < .37$ on an orbit-by-orbit basis.

2. Limits on Spectral-Intensity Correlation

We have accumulated data at $E > 6$ keV (E_{High}) and $E < 6$ keV (E_{Low}) on an 82 second basis. We then sorted the data into 10 intensity bins on the basis of E_{Low}. In Figure 5 we plot the average of E_{High} whenever E_{Low} was within the prechosen bin limits, along with lines which correspond to power law spectra of slopes $\Gamma = 2.0$, 1.75 and 1.50 with N_H fixed at 4.3×10^{22} cm^{-2}. The data are all consistent with the $\Gamma = 1.75$ line. We note that each point in Figure 5 represents an independent measure of the power law index. We conclude that there is no intensity related spectral variability with an upper limit on a change in spectral index of $\Delta\Gamma < .30$. (This method of analysis could hide possible variability if the same intensity state has different spectral indices and if these values scatter about a given mean value which is also characteristic of the total time averaged spectrum.)

3. Spectral Cross-Correlations

A defect of the prior two methods is the relatively large bin sizes (30 minutes and 82 seconds), necessitated by the relatively low flux, compared to the characteristic variability time of ~ 100 seconds. The cross-correlation function allows one to test the entire data stream on shorter timescales to see whether the softer photons systematically lead or lag the hard ones. We report here the result of two cross-correlation analyses, one designed to minimize the detectable timescale, and the other to maximize the difference between the selected energy bands.

Cross correlation of the total flux from the MED (which is sensitive to photons with a mean energy of $\bar{E}$ = 5.46 keV for the NGC 6814 spectrum) with the total flux from HED3 ($\bar{E}$ = 8.67 keV) shows that the MED leads HED3 by 6.3 ± 3.3 sec for a bin size of 15.3 sec (see Appendix B). We also cross correlated photons of energy < 6 keV ($\bar{E}$ = 5.17 keV) with photons of energy > 6 keV ($\bar{E}$ = 12.50 keV). For this analysis we used a bin size of 41 sec since this made the errors due to Poisson noise similar to those in the MED vs HED3 analysis. We found that the > 6 keV photons lead the softer photons by 4.1 ± 9.6 sec.

4. Spectral Variability of a Resolved Event

The flux change shown in Figure 2 has sufficient statistics to examine spectral variability within a given event. As can be seen in the middle panel the effective spectral index Γ did not change ($\Delta\Gamma < .30$) during this event despite the five fold change in source flux. These data also rule out variation in X-ray column as the origin of the short term variability. Due to the low flux the hardness ratios are binned in 82 second bins and thus we cannot comment on spectral variability on the shorter timescale indicated in the previous section. We conclude that, for this one event, spectral variability does not occur on the characteristic time of intensity

variability.

V. DISCUSSION

The rapid variability observed in NGC 6814 can place strong constraints on the physical processes producing the X-ray flux and the environment in which it is produced. We shall discuss with respect to the NGC 6814 data general constraints, and limits we can place on "standard" X-ray emission mechanisms.

A. General Considerations

The average luminosity of NGC 6814 is $1.1 \times 10^{43}\ h^{-2}$ ergs/sec in the 2-20 keV band where h is Hubble's constant measured in units of 50 km/sec/Mpc. Since the amplitude of the variability is quite large we will assume that the change in luminosity is greater than 10^{43} ergs/sec. If the X-ray spectrum extends out to $\sim$ 500 keV, as does the X-ray emission from Cen-A (Baity et al. 1981), then the average luminosity is $\sim 4.7 \times 10^{43}\ h^{-2}$ erg/sec.

If NGC 6814 is powered by accretion onto a single compact object, then we can set a firm upper limit on the mass of this object by requiring that the fluctuation time be longer than the light travel time across the Schwarzschild radius. This gives

$$M \lesssim \frac{c^3 \Delta t}{2G} \simeq 1 \times 10^7\ M_\odot$$

for $\Delta t = 100$ sec. On the other hand, we find that

$$M > 9 \times 10^4\ M_\odot / h^2$$

by requiring that the luminosity not exceed the Eddington limit. Without a

detailed model we cannot restrict the mass range any further. As we will see though, a 10^6 $M_\odot$ object is consistent with thermal Compton models.

Using the Fabian and Rees (1979) relation given in the introduction with $\Delta L > 10^{43}$ erg/sec and $\Delta\tau_{min} \sim 100$ sec, we find that $\eta > 5\%/h^2$. However, if the variations extend out to 500 keV then $\eta \sim 25\%/h^2$. If one requires $\eta \leq 10\%$ then $h \sim 2$. Conversely, if $h \sim 1$ then one must consider models that allow high efficiencies (Thorne 1974) or argue that one of the assumptions used in deriving the Fabian and Rees relation is violated. This could imply either non-spherical geometry, relativistic bulk motions, or that the source of the X-ray flux is not directly due to accretion.

B. Emission Mechanisms

1. Synchrotron Radiation and Synchrotron Self-Compton Emission

If the X-ray flux is produced by relativistic particles in a "steady state" type process via synchrotron emission, or synchrotron self-Compton (SSC) emission, then one requires that the particles "live" long enough to fill the emitting region.

The lifetime of a relativistic electron against Compton losses is $\tau_c \approx \frac{2\times10^7 \text{ sec}}{\gamma u}$, where the energy of the electron is $\gamma m_e c^2$ and u is the energy density of the photon field. For $L \sim 1.1 \times 10^{43}$ ergs/sec and a size $R \sim c\Delta\tau \sim 100$ light seconds, $u \sim 2 \times 10^7$ erg/cm^3. Therefore $\tau_c \approx \gamma^{-1}$ seconds. In order to produce X-rays via the synchrotron process one needs $\gamma^2 B \gtrsim 6 \times 10^{11}$ (where B is the magnetic field in gauss). For "reasonable" values of B ($\lesssim 10^4$ gauss) one needs $\gamma \gtrsim 10^4$. Therefore for these particles $\tau_c < 1 \times 10^{-4}$ seconds. If the X-rays are produced by a single Compton scattering off some photon population characterized by a frequency ν_1 then $\nu_x \sim \gamma^2 \nu_1$ (Jones, O'Dell and Stein 1974). If we assign ν_1 in the range 10^9 - 10^{15} Hz (radio to optical photons), $\gamma \sim 10^{4.5}$ -

$10^{1.5}$ which gives Compton loss lifetimes of $10^{-1.5}$ - $10^{-4.5}$ seconds.

All these timescales are much less then the light travel time across the emitting region. We conclude that synchrotron and SSC models, without continual injection and/or reacceleration and/or relativistic bulk motion, cannot work.

Cavaliere and Morrison (1980) have considered a model in which the particles are continually reaccelerated and in which the radiation rate is controlled by the acceleration rate. Their model, for the parameters measured in this paper, implies electron densities $n_e \sim 1 \times 10^9$ and B fields $\sim$ 20 gauss for the case in which the X rays are primarily due to Compton interactions and the optical photons are due to synchrotron radiation, a rather higher value for n_e and a lower value of B than Cavaliere and Morrison found for NGC 4151 or 3C273.

2. Thermal Bremsstrahlung and Blackbody Radiation

The luminosity from an optically thin sphere emitting X-rays due to thermal bremsstrahlung at a temperature of T is

$$L \sim 2.4 \times 10^{-27} T^{1/2} n_e^2 V \text{ erg/sec}$$

where V is the volume of the source region and n_e is the electron density. For $T \lesssim 10^8$ K (as required by the spectral fits (Mushotzky et al. 1980)) one requires $n_e \sim 1 \times 10^{14}$ cm^{-3} for $V \sim 1 \times 10^{38}$ cm^3. This gives an optical depth to Thompson scattering $\tau \sim n_e \sigma \ell \sim 200$. Therefore our initial assumption of optically thin emission cannot be correct and the output spectrum must be optically thick in shape if the X-rays originate in a sphere of hot gas. However the X-ray spectrum does not have this shape; therefore, we conclude that the X-ray emission without Compton amplification cannot be purely thermal in character.

3. Thermal-Compton Models

Although simple accretion with thermal emission can explain the source of power, we need a more exotic emission mechanism to be consistent with both the spectrum and the rapid variability. Another X-ray source that shows rapid time variations in addition to a power law X-ray spectrum is Cyg X-1. We will now consider models originally constructed to explain Cyg X-1 but scaled up to $L = 10^{43}$ ergs/sec.

The more successful models have involved unsaturated Comptonization. For this mechanism to function the source must consist of a cloud of hot electrons with an optical depth to electron scattering τ_{es} less than a few and a copious source of soft "seed" photons. Under these conditions soft photons entering the cloud can be up-scattered in energy to X-rays, but do not spend enough time in the cloud to come into thermal equilibrium with the electrons. Shapiro et al. (1976) and Katz (1976) showed that the resultant spectrum is a power law for energies below kT_e with an exponential fall-off at higher energies. Pozdnyakov et al. (1979) and Takahara (1980) found qualitatively similar results in Monte Carlo calculations for a wide range of temperatures and optical depths. The location of the roll over is somewhat model dependent with the result from Shaprio et al. occurring at the lowest temperatures. However, all of the calculated spectra roll over significally by 3 kT_e. There is no evidence for either a roll over or a Wien peak in the spectrum of NGC 6814 or of any other AGN where spectra have been measured to higher energies. This implies that $kT_e > 15$ keV in NGC 6814. Since Cen-A, the source with the best determined spectrum, has a power law out to ~ 500 keV (Baity et al. 1981) it is possible that $kT_e \gtrsim 300$ keV.

For unsaturated Compton models τ_{es} and kT_e are related by

$$\tau_{es} = \left(\frac{650\ keV}{kT_e}\right)^{1/2} - 2/3 \qquad (1)$$

(Sunyaev and Titarchuk 1979), for $\Gamma = 1.7$ as measured for NGC 6814. Using Equation 1 we compute that $\tau_{es} = 4.0, 1.9, .8$ for electron temperatures of 30, 100 and 300 keV. Notice that although kT_e ranges over a factor of 10 the product $(\tau_{es} \cdot kT_e)$ only changes by a factor of 2. This will be useful below.

In any mechanism involving inverse Compton scattering, the harder photons are on the average scattered more times than the softer photons. Lightman et al. (1978) pointed out that this implies that the harder photons spend more time in the source region, causing the more energetic photons to lag the soft during fluctuations. Lightman et al. suggested that the rise time of a flare t_m, measured at energy E, should be given by

$$t_m = t_R\ A\ \ln(E/E_s) \qquad (2)$$

where $t_R = R/c$ (size of source region), A is a constant on the order of unity and E_s is the energy of the original soft photons. More detailed calculations (Payne 1980; Lightman and Rybicki 1979) have shown that

$$A = \frac{m_e c^2}{\tau\ kT_e\ (3 + 2\alpha)} \qquad (3)$$

where $\tau = N\sigma_T R$ and α is the power law index of the persistent source ($\alpha = \Gamma - 1$). Since $(\tau \cdot kT_e)$ appears as a product we can easily estimate A to within a factor of 2. If we use $kT_e \sim 100$ keV, we find $A \sim .6$.

In equation 2, t_m is unobservable since it is measured from the (unobserved) injection time of the original soft photons. We set $t_m = (1+f)t_o$ where t_o is the observed rise time of the flare and f is model dependent but only a slowly varying function of E_s. Solving for t_R gives

$$t_R = \frac{(1+f)\ t_o}{.6\ \ln(E/E_s)}. \qquad (4)$$

Before we can go on we must estimate E_s. Lightman et al. (1978) suggested measuring the rise time of a flare in two energy windows and then determining the ratio of rise times

$$D = \frac{t_{m1}}{t_{m2}} = \frac{\ln(E_1/E_s)}{\ln(E_2/E_s)}. \qquad (5)$$

Solving for E_s one finds that, for $E_s < .1$ keV, E_s is proportional to E_1 and E_2 raised to large powers. Thus a small error (1%) in D can result in a factor of 10 uncertainty in E_s. In addition, equation 5 is only approximate since it uses t_m instead of the observable time t_o. An observational problem is that the statistics are not good enough to determine two different rise times in two narrow windows. Thus we are unable to determine E_s accurately, but estimating this number will not result in too large an error in t_R.

Since Seyferts are known to be strong IR sources we choose E_s =1 eV. This is consistent with the hypothesis of the soft seed photons originating in a large accretion disk which should be rather cool. We define t_o as the time for the intensity to go from .37 I_{max} to I_{max}. With $\log(E/E_s) = 3.8$ we find $f \sim 2$ using the function given by Payne (1980). Thus

$$t_R \sim 60 \text{ sec},$$

which says that the size of the source region is slightly smaller than the variation time. If we assume the peak flux comes from ~ 5 Schwarzschild radii then we estimate the mass of the compact object as

$$M \simeq \frac{c^3\ 60 \text{ sec}}{10\ G} = 1 \times 10^6\ M_\odot.$$

If the geometry is canonical Kerr then the peak X-ray flux comes from 0.8 Schwarzschild radii (Thorne 1974). For this case $M \sim 8 \times 10^6 M_\odot$.

Although it has been impossible to measure D and thus check the consistency of the unsaturated Compton model, another test can be made. Photons at E_2 ($>E_1$) should always lag photons at E_1 by an amount

$$\Delta t_m = t_{m2} - t_{m1} = A t_R \ln(E_2/E_1) . \qquad (6)$$

This equation is independent of the soft photon energy but is a function of the electron temperature. It is possible to measure Δt_m, using the cross-correlation function, for the entire data stream, not just during the rising portion of an event. Using t_R = 60 sec and A = .6 one predicts Δt_m = 30 and 17 sec for the < 6 keV vs > 6 keV and MED vs HED 3 data respectively. Recall from the observations in Section III that the measured times were -4 ± 10 sec and 6 ± 3 sec, respectively. Both of these values of the lag time are consistent with the observed lag time being 1/3 or less of the predicted value. One possibility is that t_R is smaller than our estimate of 60 sec (see below). Another point is that we are using rather broad energy windows which will "smear" the effect. Until we obtain more photons, allowing a smaller energy window, we cannot make any strong statements. However, the fact that the observed MED vs HED3 delay is in the right direction is encouraging.

Both Payne (1980) and Lightman and Rybicki (1979) predict large (and so far unobserved) spectral changes during an intensity fluctuation. We note a few reasons why we might not see such changes. First, Lightman and Rybicki suggested that one may identify the observed time for variability with the timescale for a change in the soft photon flux rather than t_R. Equation (27) of Lightman and Rybicki is then applicable. This equation predicts $n_e > 4 \times$

10^{12} cm^{-3} which would result in $t_R < 13$ sec, consistent with our upper limit. However, if we use the determination of $\Delta t_m = 6 \pm 3$ seconds and apply Equation 6 we find $t_R = 22 \pm 11$ seconds. Secondly, it is possible that the output spectrum calculated by Payne (1980) and Lightman and Rybicki (1979) is incorrect becasue they have not calculated a truly self-consistent model. Therefore, we cannot at present use our observations to critically constrain such models. Finally, it is possible that unsaturated Comptonization is not the correct model.

C. Source Lifetime

We can set an upper limit for the object's lifetime at its current luminosity by requiring that it cannot have accreted more material than its present mass at an assumed constant accretion rate. If we assume a 10% conversion efficiency of matter into radiation, consistent with some of the theoretical discussions of accretion onto a black hole (see Rees 1979 for discussion of the energetics of accretion onto black holes and see Thorne 1974 for a discussion of possible values of the efficiency), the accretion rate for NGC 6814 must be $\gtrsim .002\ M_\odot/yr$ to account for the observed luminosity. This gives a lifetime

$$\tau_L \lesssim \frac{10^6\ M_\odot}{.002\ M_\odot/yr} = 5 \times 10^8\ yrs$$

which is considerably shorter than the Hubble time. We cannot rule out the possibility that $M \gtrsim 5 \times 10^6\ M_\odot$ and that the efficiency is near 30% (Thorne 1974), in which case the source could have maintained its present luminosity for a Hubble time. If the 10% efficiency assumption is correct, one must consider alternate scenarios. Possibilities are that the object has a duty cycle of $\tau_L/t_{Hubble} \lesssim .03$ or that the high luminosity is a recent

phenomenon. We note that ~ .02 of all galaxies with M_v <-19 are active galaxies (Huchra 1977). The value of the "on" duty cycle is therefore consistent with the hypothesis that all galaxies show a Seyfert-like nature for ~ .02 of their lifetimes.

D. Why Is NGC 6814 Different?

NGC 6814 is the only AGN in the HEAO-1 A-2 sample (Tennant et al. 1981) to show such rapid variability. In this section we speculate on why this may be so. For convenience we have divided this section into two parts. First, we consider whether the same emission mechanism could account for the observed differences. Next we consider if we are observing a different emission mechanism but a "typical" galaxy. Throughout this section we will be using the fact that most active galaxies are ten times more luminous than NGC 6814. However, if the observed variations are a property of luminosity only then both NGC 4151 and Cen A should show such rapid variability but do not, at least in the HEAO-1 data.

1. Similar Emission Mechanism

The light curve for NGC 6814 differs from other objects in two ways, the magnitude of the variations and the timescale involved. Let us now consider how decreasing the amplitude of variations would affect our ability to detect variations. For a source counting rate of S and a background rate of B one can show

$$\frac{\sigma_s}{S} = k \left\{ \left(1 + \frac{B}{S}\right) \frac{1}{ST} \right\}^{1/2} \qquad (7)$$

where T is the bin size, and $k^2 = \langle \sigma_s^2/\sigma_c^2 \rangle$ is the average ratio of source variance to the counting statistics variance. For the case where σ_s is independent of time, the reduced χ^2 is a measure of $1 + k^2$. Thus equation 7

allows us to relate reduced χ^2 to the intrinsic source variance.

In order to minimize systematic errors we will compare NGC 6814 with other objects using only the counting rate from the small field of view of the xenon detector (which has only one-fourth of the total area). NGC 6814 data with a 300 sec bin size and total length of 2000 seconds gives $\chi^2_\nu = 10$. Using B = 8.7 and S = 1.4 ct/sec we find that $\sigma_s/s = 36\%$. Other sources with counting rates similar to NGC 6814 typically have $\chi^2_\nu < 2$ which implies that $\sigma_s/s < 13\%$. If other sources show similar variations then the amplitude must be reduced by at least a factor of three. A factor of three can be accounted for in a shot noise model. In this model one sees a superposition of identical shots each with height h and decay time τ occuring at a rate λ. In this case $S \propto \lambda h\tau$ and $\sigma_s^2 \propto \lambda h^2\tau$. For the case where h and τ are constant from source-to-source we find $\sigma_s/s = 1/\sqrt{\lambda} \propto 1/\sqrt{L}$. It will be possible to test if this relation holds with our data for other sources.

A χ^2 test on a variable source will be indicative of variability if the timescale for variation is greater than the bin size and less than the total sample time. The HEAO-1 pointed observations are sensitive to all timescales from 10s of seconds to $\sim$ 3 hrs. To observe longer timescales one needs to use scanning data. However, to obtain similar statistics a bin size of one to two days is required. Therefore timescales from 3 hr to 30 hr have not been adequately sampled. If we assume that the source variance is due to shot noise then it is possible that the brighter sources have the same shot rate but a longer decay time. In this case the more luminous sources would show longer timescales and again $\sigma_s/s \propto 1/\sqrt{L}$.

If rapid time variability only occurs in episodes, then our data indicate that at any one time only one object in $\sim$ 30 will be having an episode. This can be tested only by watching a large number of objects in

addition to NGC 6814 for a long period of time.

2. Different Process

In this section we assume that the X-ray emission from NGC 6814 is due to a different physical process than for other AGN's. We further assume that other sources also have a component similar to that in NGC 6814 but that for some reason it is generally not seen. Let us call the small variable component V and the larger more constant component C. We have to assume that the X-ray spectrum from V must be quite similar to the spectrum from C. Additionally we note that NGC 6814 is not unusual in its X-ray or optical properties. Thus the only obvious difference between V and C is the rapid time variability.

Consider ways in which the V component could normally be hidden. One possibility is that the C component is normally much more luminous. If this case is correct then one might expect $\sigma_s/s \propto L^{-\beta}$. This is consistent with the observation (Mushotzky et al. 1981) that on timescales > 12 hours the low luminosity sources are typically more variable.

Another way that one might hide a V component is with geometry. This is possibly supported by the fact that NGC 6814 is almost a face on object. Heckman et al. (1978) surveyed 21-cm emission from 23 Seyfert galaxies. Of this sample no other active galaxy had a smaller HI line width than NGC 6814, showing that most of the rotation is in the plane of the sky. If active galaxies send matter and or radiation out along the rotation axis then it is most likely that we would see it in NGC 6814. Even if we do not see such a "jet" directly then it might have blown a hole in the accreting gas surrounding the central object. This would allow us to see the nucleus directly whereas from other directions it would be obscurred by material accreting onto the central object.

VI. CONCLUSIONS

NGC 6814 exhibits strong X-ray variability on timescales less than 5000 seconds. The autocorrelation function shows a characteristic time of $\lesssim$ 100 seconds. There does not appear to be a strong spectral-temporal effect since any change in the spectral index is less than .35 during strong intensity variations. There is a weak indication, however, that soft photons may systematically lead hard photons by $\sim$ 10 seconds.

We compare our data with various models and conclude that, unless reacceleration or continuous injection of particle occurs, neither the synchrotron nor the synchrotron self-Compton processes can be the origin of the X-ray emission. However, we do find that our data are consistent with the general predictions of thermal-Compton models. We note that it is necessary to observe a roughly exponential rollover in the high energy end of the X-ray spectrum in order to confirm the validity of thermal Compton models of AGN's.

NGC 6814 appears to be unique. In our sample of over 30 active galactic nuclei (Tennant et al. 1981) only NGC 6814 shows rapid variability. We speculate that this might be related to its low X-ray luminosity.

ACKNOWLEDGMENTS

We thank Alan Lightman for interesting discussions, M. Elvis for communication of results prior to publication and S.S. Holt, F.E. Marshall, and P.J. Serlemitsos of the X-ray group at GSFC for their support and encouragement. We also thank the HEAO-1 scanning modulation collimator experiment and data reduction and analysis team at CFA and MIT.

APPENDIX A

DATA CONSISTENCY CHECKS

Since the rapid variability of NGC 6814 is so far unique we feel that a detailed discussion of the checks that we made will be useful.

A. Instrumental Self Checks

The Goddard Space Flight Center's A-2 experiment (Rothschild et al. 1979) is a powerful tool to conduct stability studies of X-ray sources. The instrument consists of four detectors each with two different fields of view. Usually, three of the detectors (deck) view the source while the fourth (offset) detector views background. During the NGC 6814 pointed observation, each of the three deck detectors independently saw statistically the same light curve that is shown in Figure 1, while the offset detector had a counting rate consistent with a constant for the duration of the point.

Instrumental stability is quite good and was tested during the so called "blank sky" points. A "blank sky" point occurred whenever the A-1 instrument on HEAO-1, which looks 180° from our look axis, was pointed at a source and there were no HEAO-1 sources (flux $\gtrsim 2 \times 10^{-11}$ ergs/cm^2 sec) in our field of view. Examining the look position from all A-1 pointings we found that 55 different observations were truly "blank sky" for a total observation time of 380 hours. We have analyzed the data from these points and report that only once did we see a short duration rate increase in more than one detector. This event turned out to be time coincident with a solar flare. At no time did we see a short duration rate decrease.

The rates during the "blank sky" points were analyzed with our standard

data selection flags. At no time did we see a clear indication of contamination due to particle events. Therefore, we conclude that the net contribution due to particle contamination of the background subtracted counting rate is usually less than 0.1 count/sec in each detector.

The "blank sky" points also showed that the background can differ by 4% from one point on the sky to another. Changing the background flux by 4% changes the average NGC 6814 flux by ~ 20% but does not significantly affect the shape of the light curve.

B. Source ID

Ariel-5 was first to report an X-ray source at the position of NGC 6814 (Elvis et al. 1978). Their identification was uncertain since their error box also allowed the globular cluster PAL 11, which lies about 2° away, to be the X-ray source. The HEAO-1 error box (Mushotzky et al. 1980) was aligned in such a way that it is unlikely that the cluster is the X-ray source. For the pointed observation we can rule out the cluster with 100% certainty since it was never in our small (3° x 1.5°) field of view. For a picture of the two error boxes see Mushotzky et al. (1980).

The Einstein Observatory observed the source with both the HRI and the IPC (Tananbaum 1980). The HRI showed a point source within 5" of the visible light nucleus which confirms that the galaxy is an X-ray source. The IPC showed no other sources with a flux greater than one-tenth the NGC 6814 flux in the 30' field of view (M. Elvis 1981). In addition, the IPC detected strong variability with a timescale of a few hours. Faster variations could not be detected since the count rate was only 0.07 ct/sec. We expect the IPC to detect a lower flux than HEAO-1 since it has a smaller area and it looks in a lower energy band which is affected by the low energy absorption seen in NGC 6814. We have converted the IPC counting rate into a spectral

normalization by assuming a spectrum and using the tables in Giacconi et al. (1979). We find that 0.07 IPC counts/sec correspond to a norm of 4.7, 2.2 and 9.4 photons/cm^2 ksec keV for spectra with $\Gamma = 1.75$, $N_H = 5.0$; $\Gamma = 1.50$, $N_H = 2.9$; $\Gamma = 2.0$, $N_H = 7.9$ respectively where N_H has units of 10^{22} atoms/cm^2. The three spectra represent the best fit, lower and upper 90% confidence range found by Mushotzky et al. (1980). The norm found by Mushotzky et al. for the total observation using the best fit values was 19 which is a factor 4 greater than the IPC norm assuming the same spectrum. However, if one compares the range of possible norms found for the IPC with the numbers in Tables III and IV we find that they do overlap. Thus the low IPC flux is not inconsistent with NGC 6814 being the X-ray source.

C. Aspect

HEAO-1 was designed as a scanning experiment and this has meant that the aspect solutions during a point are not as accurate as obtained during scan. The HEAO-1, A-3 experimenters generate their own aspect solutions and have kindly provided some information to us. By comparing the two aspect solutions we find that the A-2 solution can drift up to 0.3° at the end of 6 hrs. Often the solution is much better. By looking at strong constant sources we have found that errors in the GSFC provided aspect solution can introduce an apparent 10% variation in source intensity. We find that it is relatively easy to identify aspect problems since the area corrected rate is inversely proportional to the effective area. Thus although we can identify aspect errors we still cannot make any strong statements about source stability below the 10% level.

For the NGC 6814 observation we have compared the observed flux with the effective area and see no correlation. We note that many of the variations are seen in the raw counting rate. Further we have conducted the stronger

test of comparing the counting rate with look position. If the aspect is in error or a confusing source is inside the detector beam one would expect to see a similar flux whenever the spacecraft is looking at a similar positic in the sky. We see no correlation between look position and counting rate. During the rapid rate decreases in orbits one and three the spacecraft look position was moving slowly through a region it had been looking at for more than 1/2 the orbit.

APPENDIX B

NONPERIODIC SIGNAL ANALYSIS

In this appendix we will present some details of the methods used to analyze the NGC 6814 light curve. We feel that such a presentation of this is needed for several reasons. First, there are several definitions of the autocorrelation function (ACF) and several ways one can use the function. We discuss our choice and reasons. Further, application of the ACF to real data requires consideration of the effects of the data gaps, finite data trains and photon counting statistics. Finally, it is not trivial to compute the uncertainties in the derived results. This is due to the fact that the data are correlated and thus straight propagation of statistical errors can grossly underestimate the errors involved. For NGC 6814 we found that the dominant source of error arose from the finite observation length. Therefore we spend the most time discussing errors from this source.

Given a binned set of observations Y_i with statistical errors σ_i we compute the ACF from

$$\rho(u) = r(u)/r(0)$$

where

$$r(u) = \frac{1}{N} \sum_{i=1}^{N-u} \frac{(Y_i - \bar{Y})\,(Y_{i+u} - \bar{Y})}{\sigma_i\,\sigma_{i+u}} \qquad B1$$

where $\bar{Y}$ is the weighted mean and u is the lag time measured in bins. Jenkins and Watts (p172f) show that using 1/N instead of 1/(N-u) in the definition of r(u) introduces a bias into the estimator of the ACF for large u, but the biased estimator has lower mean square error. Equation B1 shows that the

weighted ACF is directly related to reduced χ^2. Thus χ^2_ν should differ from 1.0 by many sigma in order to determine a statistically significant ACF. This becomes apparent as one goes to smaller bin sizes since the statistical errors dominate and so χ^2_ν becomes less significant. We have found that for practical purposes the minimum bin size occurs when χ^2_ν differs from 1.0 by $\sim$ 5 sigma where sigma is given by $\sqrt{(2/N)}$. For smaller bin sizes noise dominates the ACF.

We now consider data gaps, which can be of two types, short (a few minutes) or long ($\sim$ 1/2 hour). Short gaps have relatively little affect on the ACF, which means that any reasonable method of gap filling should work. We gap fill by replacing the missing data with the average. This method will not introduce any false peaks into the ACF, since the ACF is only sensitive to deviations from the average.

The long gaps present a somewhat different problem. One could again gap fill with the average but this is equivalent to assuming that the entire data stream is a sample of a stationary stochastic process. We are uncertain whether this is a reasonable assumption. In particular, the large change in the average flux from orbit-to-orbit will increase the short term correlations. If we assume that we are dealing with a stochastic process superimposed on top of a time varying mean, then we can detrend the data to concentrate on the short term variations. We "detrend" by subtracting the orbital mean from each orbit's worth of data. Another method to treat large gaps is to simply not cross the gap. This means that one computes the ACF for only one orbit at a time. We prefer this method since it allows comparisons to be made between different observations.

The dominant source of error in the timescales reported here is due to the finite length of the data stream. Crudely put, to measure a

timescale τ one needs an observation with a length of many (~ 10) τ. To estimate the error introduced by the finite data length we have generated simulated data streams using a first order autoregressive process (see Jenkins and Watts 1968). For a first order process a data point y(I) is generated by

$$y(I) = \alpha y(I-1) + Z \qquad B2$$

where $|\alpha| < 1$ and Z is a random number with mean $\langle Z \rangle$ and variance, var(Z). The mean and variance for the y's are given by

$$\langle y \rangle = \frac{\langle Z \rangle}{1-\alpha}$$
$$\text{var}(y) = \frac{\text{var}(Z)}{1-\alpha^2} \qquad B3$$

The ACF for the first order process is an exponential with decay time $\tau = -1.0/\ln(\alpha)$. Since the ACF is independent of the various moments of the data, the errors in the timescale will also be independent of the moments. The autoregressive process is useful since it is easy to compute and allows one to separate easily the timescale parameter α from the various moments. The shot noise model also allows this separation.

The maximum likelihood estimate for α is $\rho(1)$ (Jenkins and Watts 1968). Although one feels that it is possible to obtain a better result by using more than one point, numerical tests have shown that the best estimate is $\rho(1)$ alone. It is possible to estimate the uncertainty in $\rho(1)$ from

$$\sigma^2 \approx (1 - \rho(1)^2)/L \qquad B4$$

(Box and Jenkins 1976) where L is the number of points in the longest, continuous data segment. We numerically tested the estimate for σ for various L's and with $\alpha = .9$ and believe the estimate is quite good for $L > 100$. To allow for photon counting noise, which is not considered above, and any other systematic effects the errors reported are 50% larger than the value given by B4. It is possible for $\rho(1) + 1.5\sigma$ to exceed unity. This tells us that the timescale could be as long as the obsevation, which is reported as $+\infty$ in Table II.

For any finite observation of a varying signal, the ACF must show periods of negative correlations. We can estimate the lag time t_z when the ACF crosses zero by finding the time when $\rho(t)$ equals 1.5σ. This gives

$$t_z \sim (\tau/2)\ \ln(2N/3(1-\rho(1)^2)) \qquad \text{B5}$$

For orbits one and two, $N \sim 200$ and $\tau \sim 100$ sec, equation B5 predicts $t_z = 330$ sec. The observed time for both orbits was 250 secs. This shows only that the zero crossing time is closely related to the observation length.

Finally, Weisskopf et al. (1975) pointed out that photon counting noise affects the normalization of the ACF for non-zero lags. Their procedure for generating the correct autocorrelation function $\rho_c(u)$ was to multiply by a correction factor F(u); i.e., $\rho_c(u) = F(u)\ \rho(u)$. The function that we used has two values given by

$$F(u) = \begin{cases} 1, & \text{for } u = 0 \\ \dfrac{\chi^2}{\chi^2 - N}, & \text{for } u \neq 0, \end{cases} \qquad \text{B6}$$

where χ^2 is the standard chi-square computed assuming the N data points have a constant mean. For NGC 6814, F was typically in the range 1.5 to 2.5.

Correcting for photon noise means that the best estimate for τ is no longer $\rho(1)$. To be consistent we determined τ by making a least squares fit to $\ln(\rho(u))$ for lags in the range 0 to τ. This procedure is only slightly affected by data binning and for the most part gave estimates of τ consistent with $\rho(1)$.

The spectral cross-correlation function CC(u) is based on equation B1 but now using two different sets of Y values. The cross-correlation lag time t is given by the ratio

$$CC(1)/CC(-1) = \exp(2t/\tau) \qquad (B7)$$

if t is less than the bin size. Notice that the ratio CC(1)/CC(-1) does not need to be corrected for photon noise and also is independent of a bias (to first order). To allow for the smaller expected error we apply equation B4 with L replaced by N, the total number of data points used in computing the cross-correlation function. We use B4 to estimate the percentage error in $\rho(1)$ and argue that the error in the ratio is twice the percentage error in $\rho(1)$. Since the ratio is independent of the bin size we used rather large bins to minimize Poisson errors.

TABLE 1

NGC 6814

ORBIT	MEAN FLUX cts/cm^2 ksec	χ^2 (82 sec bins)	DOF
1	5.6	279.6	21
2	2.1	67.9	23
3	4.8	77.2	11
4	2.5	12.3	9
5	2.9	35.9	6

TABLE 2

AUTOCORRELATION FUNCTION RESULTS

ORBITS USED	DETREND	TIMESCALE (SEC)
1	No	85^{+60}_{-25}
2	No	$230^{+\infty}_{-130}$
1-5	No	$248^{+\infty}_{-110}$
1-5	Yes	101^{+59}_{-26}

TABLE 3

NGC 6814 SPECTRAL FITS

ORBIT	A	Γ	N_H ($\times 10^{22}$)	χ^2
1	20.4	$1.67^{+.23}_{-.21}$	$5.4^{+3.2}_{-2.2}$	1.5
2	7.2	$1.68^{+.46}_{-.35}$	$2.5^{+3.8}_{-2.5}$	4.8
3	7.7	$1.35^{+.23}_{-.21}$	$2.5^{+2.5}_{-2.3}$	14.0
4	5.7	$1.55^{+.51}_{-.07}$	$0^{+3.6}$	7.7
5	6.0	$1.58^{+.52}_{-.10}$	$0^{+3.8}$	5.3

TABLE 4

NGC 6814 SPECTRAL FITS

(ABSORPTION FIXED AT 4.3×10^{22})

ORBIT	A	Γ
1	16.5	$1.59^{+.07}_{-.07}$
2	11.2	$1.87^{+.19}_{-.16}$
3	11.1	$1.49^{+.10}_{-.09}$
4	18.9	$2.06^{+.24}_{-.21}$
5	20.4	$2.07^{+.27}_{-.22}$

REFERENCES

Baity, W.A. et al. 1981, Ap. J. 244, 429.

Box, G.E.P., and Jenkins, G.M. 1976, Time Series Analysis: Forecasting and Control (San Francisco: Holden-Day), p. 34.

Cavaliere, A., Morrison, P. 1980, Ap. J. (Letters) 238, L63.

Cavallo, G., Rees, M.J. 1978, MNRAS 183, 359.

Delvaille, J.P., Epstein, A., Schnopper, H.W. 1978, Ap. J. (Letters) 219, L81.

Elvis, M., Maccacaro, T., Wilson, A.S., Ward, M.I., Penston, M.V., Fosbury, F.A.E., and Perola, G.C. 1978, MNRAS 183, 129.

Elvis, M. 1981, private communication.

Fabian, A.C. 1979, Proc. R. Soc. London A 366, 449.

Fabian, A.C., Rees, M.J. 1979, Proc. IAC/Cospar Symp. on X-ray Astronomy, p. 381, ed. W.A. Baity and L.E. Peterson, Pergamon Press.

Giacconi, R. et al. 1979, Ap. J. 230, 540.

Heckman, T.M., Balick, B., Sullivan, W.T. 1978, Ap. J. 224, 745.

Huchra, J.P. 1977, Ap. J. Suppl. 35, 171.

Jenkins, G.M., and Watts, D.C. 1968 Spectral Analysis and Its Applications (San Francisco: Holden-Day).

Jones, T.W., O'Dell, S.L., Stein, W.A. 1974, Ap. J. 188, 353.

Katz, J. 1976, Ap. J. 206, 910.

Lightman, A.P., Giacconi, R., Tananbaum, H. 1978, Ap. J. 224, 375.

Lightman, A.P., Rybicki, G.B. 1979, Ap. J. 232, 882.

Marshall, F.E., Becker, R.H., Holt, S.S., and Mushotzky, R.F. 1981, BAAS 12, 796.

Mushotzky, R.F., Marshall, F.E., Boldt, E.A., Holt, S.S., and Serlemitsos, P.J. 1980, Ap. J. 235, 361.

Mushotzky, R.F., Swank, J.H., Boldt, E.A., Holt, S.S., and Serlemitsos, P.J.

1981, in preparation.

Payne, D.G. 1980, Ap. J. 237, 951.

Pozdnyakov, L.A., Sobol, I.M., Syunyaev, R.A. 1979, Sov. Astron. Lett. 5, 149.

Rees, M. 1979, X-Ray Astronomy, ed. R. Giacconi and G. Setti (D. Reidel, pg. 339.

Rothschild, R., et al. 1979, Space Science Instrumentation 4, 265.

Shapiro, S.L., Lightman, A.P., and Eardley, D.M. 1976, Ap. J. 204, 187.

Sunyaev, R.A., Titarchuk, L.G. 1980, Astron. Astrophys. 86, 121.

Tananbaum, H. 1980, X-Ray Astronomy, ed. R. Giacconi and G. Setti (D. Reidel), pg. 291.

Tananbaum, H., Peters, G., Forman, W., Giacconi, R., and Jones, C. 1978, Ap. J. 223, 74.

Tennant, A.F., Mushotzky, R.F., Swank, J.H., and Boldt, E.A. 1981, in preparation.

Thorne, K.S. 1974, Ap. J. 191, 507.

Takahara, F. 1980, Prog. Theor. Phy. 63, 1551.

Weisskopf, M.C., Kahn, S.M., Sutherland, P.G. 1975, Ap. J. (Letters) 199, L147.

FIGURE CAPTIONS

Figure 1 - The X-ray flux from NGC 6814 as a function of time for the first three spacecraft orbits. Data from both MED and HED3 were added together to construct this curve, giving an effective bandwidth of 3-20 keV. The bin size is 83 sec. Zero corresponds to April 28.00 (UT), 1978.

Figure 2 - a. Enlarged section of the NGC 6814 light curve plotted in Fig. 1. Time of zero seconds corresponds to 24 minutes in Fig. 1. For this figure the bin size was 20.48 sec. The data point at t = 500 sec occurred during a data drop out and so does not exist.

b. The hardness ratios defined as > 6 keV flux divided by the < 6 keV flux in HED 3 during the event shown in Fig. 2a. The hardness ratio was computed every 82 sec. The values of Γ for a given hardness ratio are indicated as straight lines labeled by the value of Γ.

c. The counting rate for HED 1 during the event shown in Fig. 2a. The HED 1 field was offset by 6° from MED and HED 3 and so was monitoring the background. For the data shown χ^2 was 42.06 for 42 degrees of freedom.

Figure 3 - a. The ACF function for orbits 1-5.

b. The natural logarithm of the ACF shown in 3a.

c. The "detrended" ACF for orbits 1-5.

d. The natural logarithm of 3σ.

Figure 4 - The photon index computed for each orbit is plotted as a function of the average flux during that orbit. We have fixed the absorption at N_H = 4.3×10^{22} atoms in the line of sight. The point near 9×10^{-11} erg/cm^2 occurred during orbit 3 where the spectral fit was unacceptable. Thus the one sigma error shown may be underestimated.

Figure 5 - The average hard flux is plotted whenever the soft flux was within a certain range. The line labeled $\Gamma = 1.75$ is the best fit line to the data. The fact that the line does not go through the origin indicates that the background subtracted was slightly in error. If the shape of the spectrum is constant during an intensity change then the data should lie along a line.

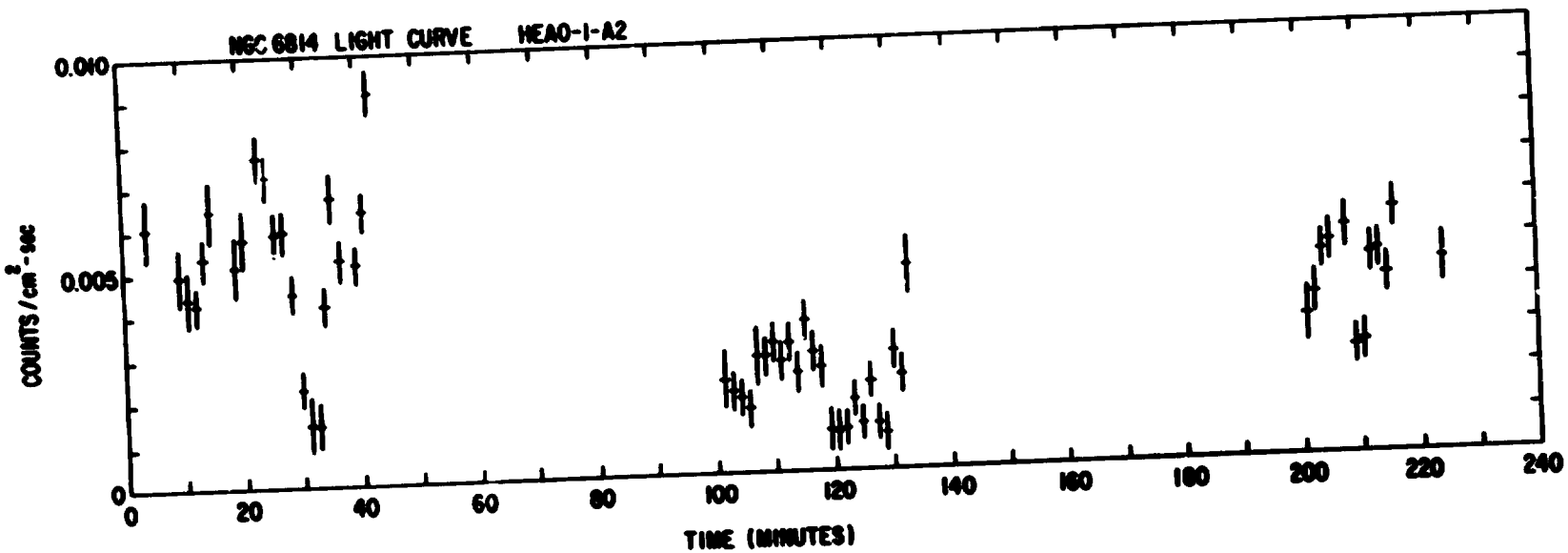
NGC 6814 LIGHT CURVE HEAO-1-A2
0.010
0.005
0
COUNTS/cm²-sec
0
20
40
60
80
100
120
140
160
180
200
220
240
TIME (MINUTES)

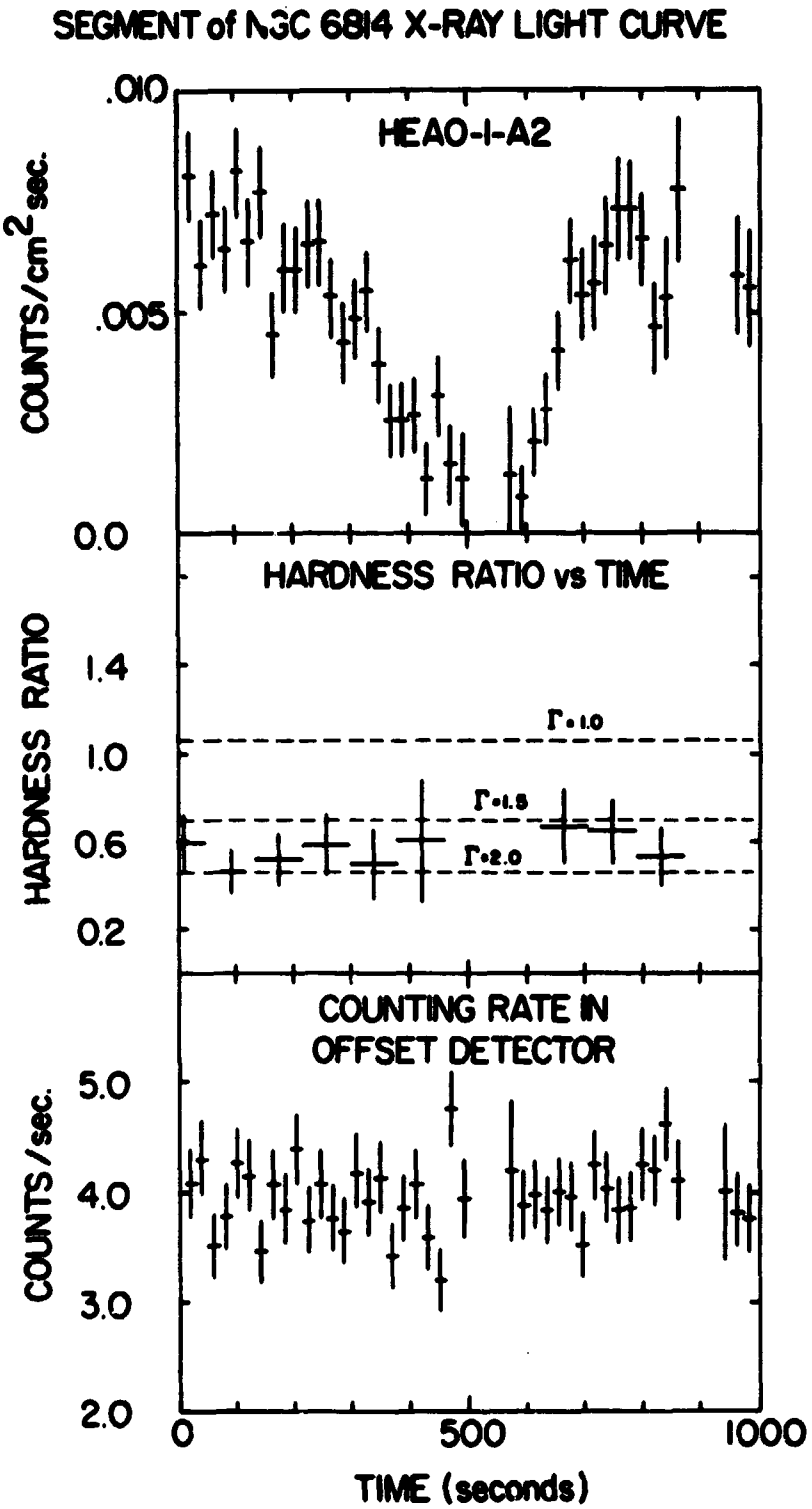
SEGMENT of NGC 6814 X-RAY LIGHT CURVE
HEAO-I-A2
COUNTS/cm² sec.
.010
.005
0.0
HARDNESS RATIO vs TIME
HARDNESS RATIO
1.4
1.0
0.6
0.2
Γ=1.0
Γ=1.5
Γ=2.0
COUNTING RATE IN
OFFSET DETECTOR
COUNTS/sec.
5.0
4.0
3.0
2.0
0
500
1000
TIME (seconds)

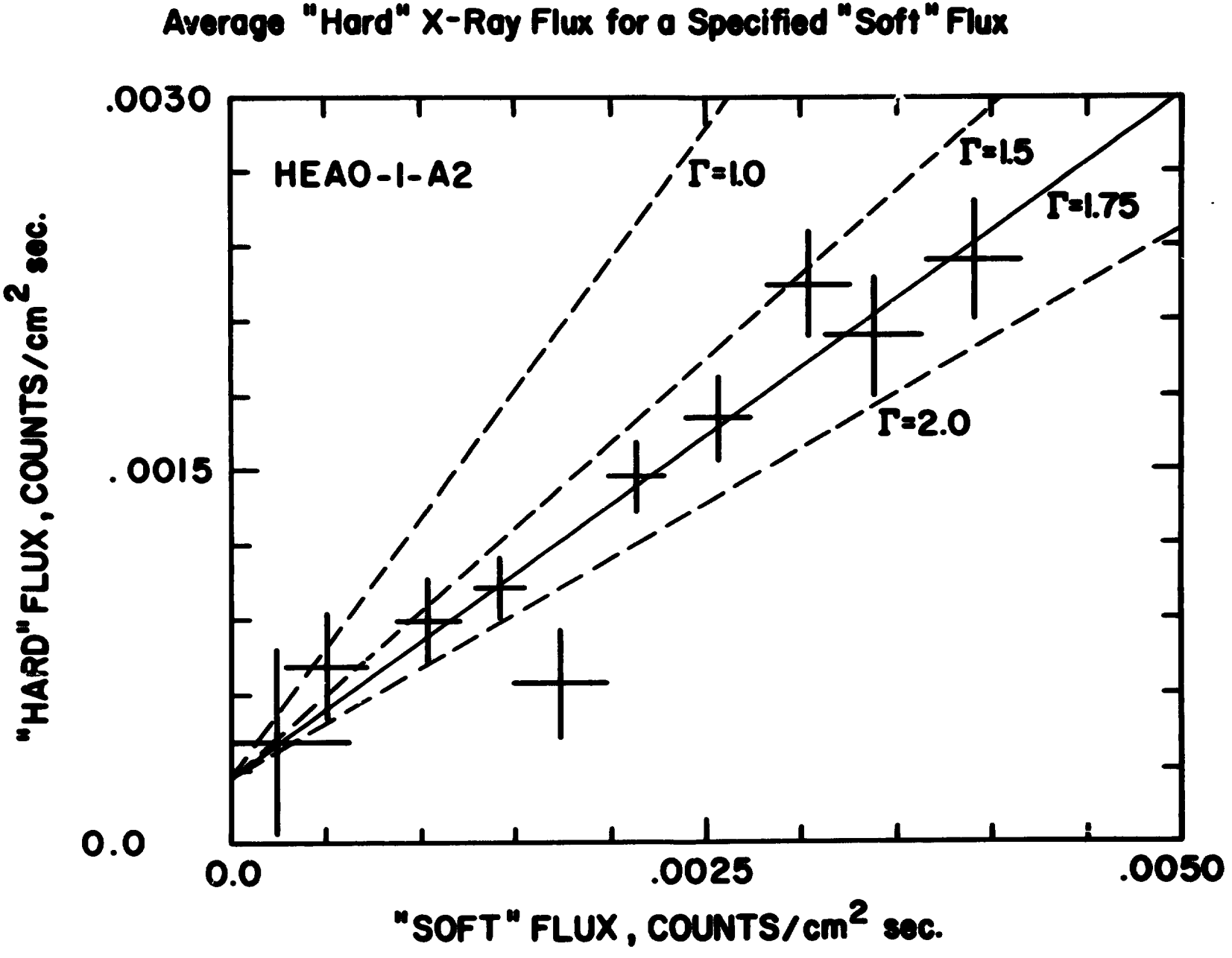
Average "Hard" X-Ray Flux for a Specified "Soft" Flux
.0030
.0015
0.0
HEAO-1-A2
Γ=1.0
Γ=1.5
Γ=1.75
Γ=2.0
"HARD" FLUX, COUNTS/cm² sec.
0.0
.0025
.0050
"SOFT" FLUX, COUNTS/cm² sec.

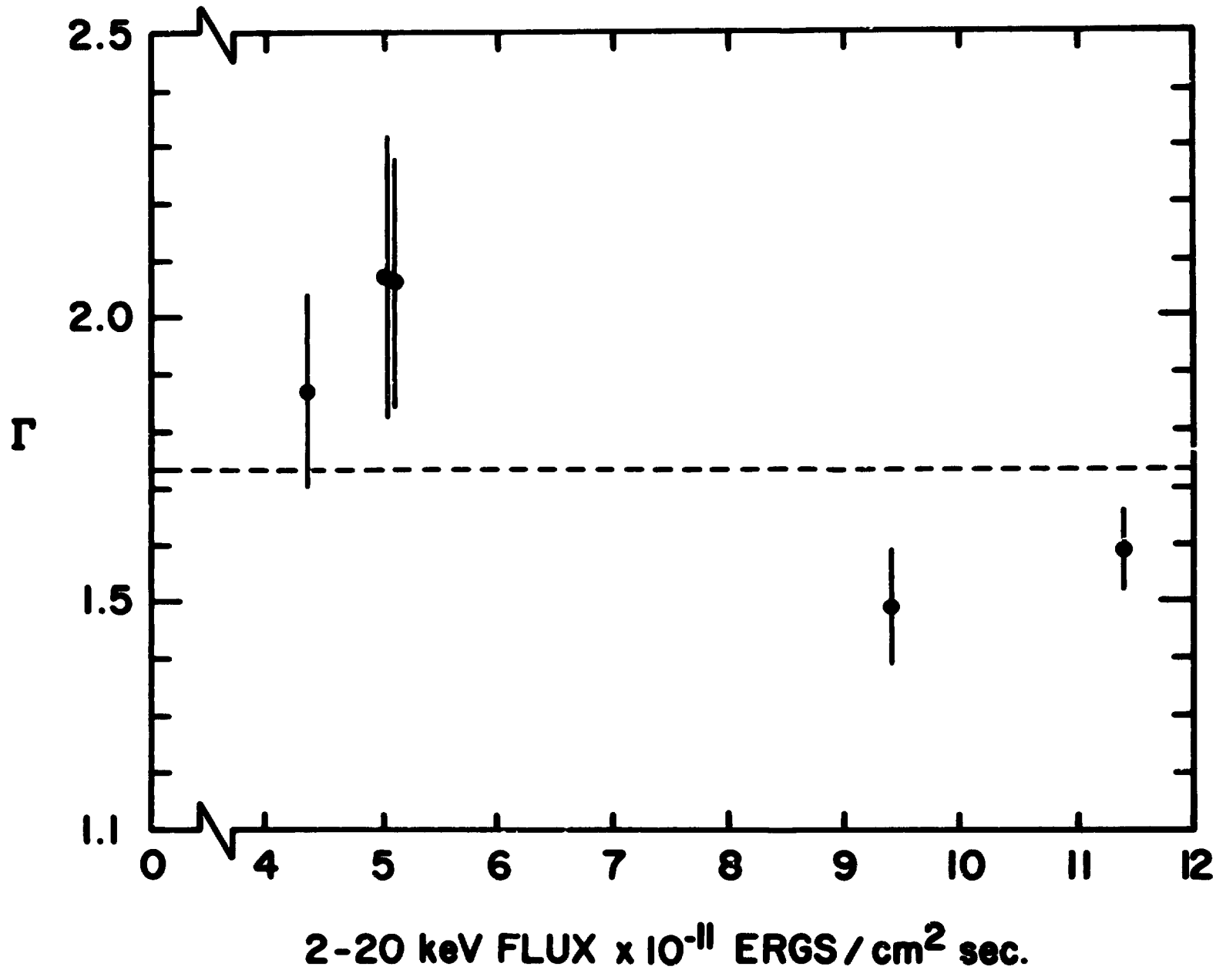
Power Law Index vs Flux (Orbital Averages)
2.5
2.0
1.5
1.1
Γ
0
4
5
6
7
8
9
10
11
12
2-20 keV FLUX x 10^-11 ERGS / cm^2 sec.

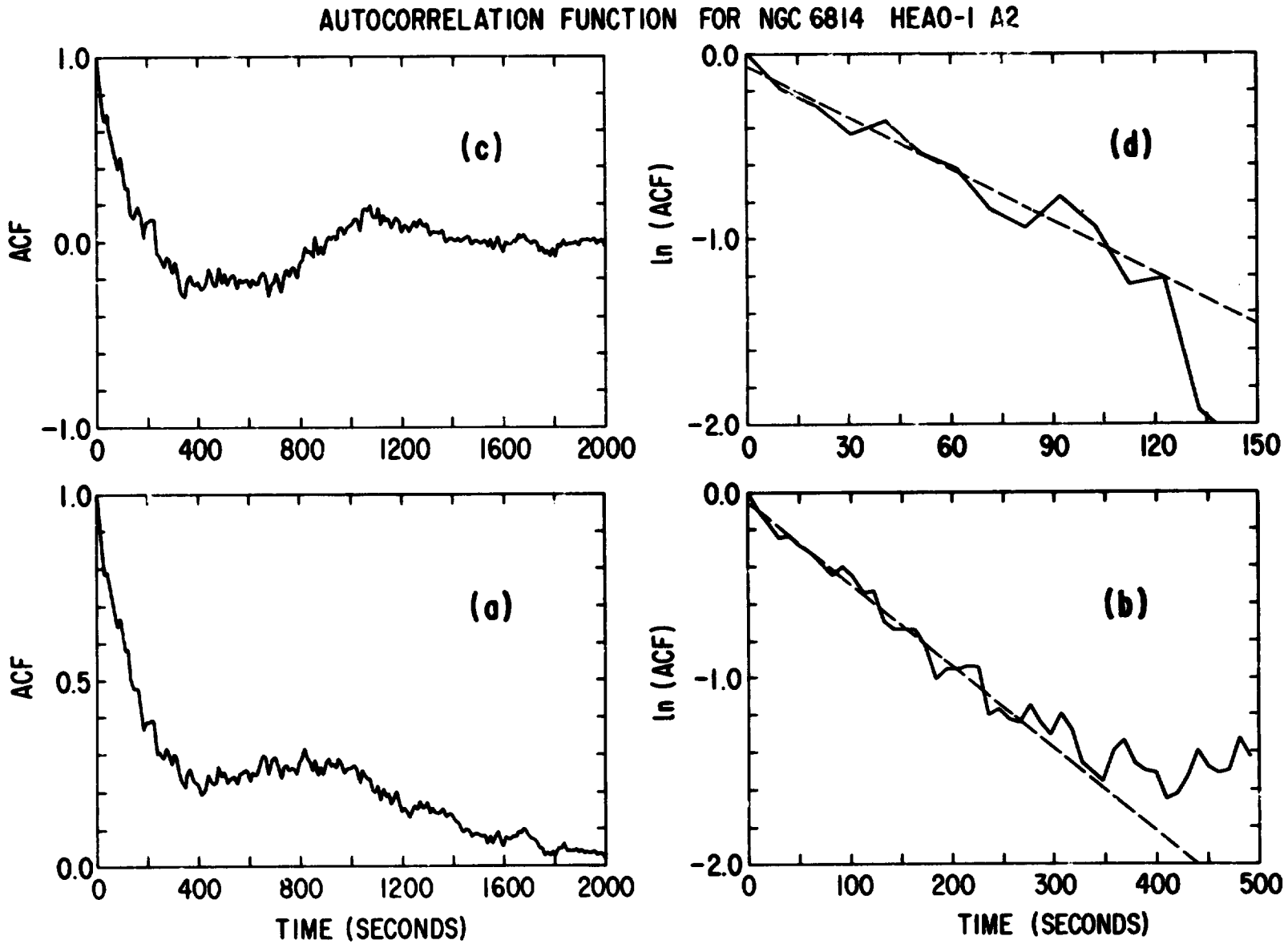
AUTOCORRELATION FUNCTION FOR NGC 6814 HEAO-1 A2
(c)
(d)
(a)
(b)
ACF
ln (ACF)
TIME (SECONDS)
1.0
0.0
-1.0
0.5
-2.0
0
400
800
1200
1600
2000
30
60
90
120
150
100
200
300
500